

Zeitschrift:	Bulletin des Schweizerischen Elektrotechnischen Vereins, des Verbandes Schweizerischer Elektrizitätsunternehmen = Bulletin de l'Association suisse des électriciens, de l'Association des entreprises électriques suisses
Herausgeber:	Schweizerischer Elektrotechnischer Verein ; Verband Schweizerischer Elektrizitätsunternehmen
Band:	75 (1984)
Heft:	23
Artikel:	Small Electric Machines
Autor:	Kreuth, H. P.
DOI:	https://doi.org/10.5169/seals-904519

Nutzungsbedingungen

Die ETH-Bibliothek ist die Anbieterin der digitalisierten Zeitschriften auf E-Periodica. Sie besitzt keine Urheberrechte an den Zeitschriften und ist nicht verantwortlich für deren Inhalte. Die Rechte liegen in der Regel bei den Herausgebern beziehungsweise den externen Rechteinhabern. Das Veröffentlichen von Bildern in Print- und Online-Publikationen sowie auf Social Media-Kanälen oder Webseiten ist nur mit vorheriger Genehmigung der Rechteinhaber erlaubt. [Mehr erfahren](#)

Conditions d'utilisation

L'ETH Library est le fournisseur des revues numérisées. Elle ne détient aucun droit d'auteur sur les revues et n'est pas responsable de leur contenu. En règle générale, les droits sont détenus par les éditeurs ou les détenteurs de droits externes. La reproduction d'images dans des publications imprimées ou en ligne ainsi que sur des canaux de médias sociaux ou des sites web n'est autorisée qu'avec l'accord préalable des détenteurs des droits. [En savoir plus](#)

Terms of use

The ETH Library is the provider of the digitised journals. It does not own any copyrights to the journals and is not responsible for their content. The rights usually lie with the publishers or the external rights holders. Publishing images in print and online publications, as well as on social media channels or websites, is only permitted with the prior consent of the rights holders. [Find out more](#)

Download PDF: 14.01.2026

ETH-Bibliothek Zürich, E-Periodica, <https://www.e-periodica.ch>

Small Electric Machines

H. P. Kreuth

Small machines account for about 25% of the total production value of electrical machines. The paper presents a survey of the main development fields with an accent on magnetic materials, on the stability problems of permanent-magnet motors and on the torque of brushless DC motors.

Kleinmaschinen machen etwa 25% des gesamten Produktionswertes der elektrischen Maschinen aus. Der Aufsatz gibt einen Überblick über die wichtigsten Entwicklungsbereiche mit Schwerpunkten auf den magnetischen Materialien, auf den Stabilitätsproblemen von Motoren mit Permanentmagneten und auf dem Drehmoment von kollektorlosen Gleichstrommotoren.

Les petites machines font environ le quart de la valeur de production de toutes les machines électriques. L'article présente une vue d'ensemble des champs de développement principaux, en mettant l'accent sur les matériaux magnétiques, sur les problèmes de stabilité des moteurs à aimants permanents et sur le moment des machines à courant continu sans collecteur.

This paper has been presented as a survey lecture at the International Conference on Electrical Machines ICEM'84 at Lausanne.

Author's address

Dr. H. P. Kreuth, Chef der Techn. Berechnung, Elektromotorenwerk Würzburg, Siemens Aktiengesellschaft, Postfach 6429, D-8700 Würzburg 1.

1. The market of small machines

Electric machines with a power input up to $P_1 = 375$ W are considered as *small machines* or *fractional horsepower machines*. In highly industrialized countries, their production value reaches 25% of the total production value of electric machines. In figure 1 the production output and production value of the Federal Republic of Germany in 1982 are shown. Small machines are mass-produced on a high level of mechanization and even automation, they are tailor-made products and undergo frequent redesign. The representative life cycle is about five years with consequently high research and development costs.

About 60% of the produced units are DC motors with commutator or brushless DC motors and have permanent-magnet excitation. Therefore, and because of technological problems arising from the small physical size of these motors, the materials constituting the magnetic circuit play an important role.

The input range $375 \text{ W} \leq P_1 \leq 10 \text{ kW}$ covers another share of 35% of the total production value, mostly 3-phase asynchronous motors and DC motors for industrial drives. Therefore more than half of the production value of electric machines is to be found in the low-power area.

2. Magnetic Materials

Since 1960 the characteristics of permanent magnets have been improved significantly and nowadays they offer such a level of air gap induction of small machines that they are more economical than electromagnetic excitation (fig. 2). A new family of materials, both with cobalt and iron, has recently gone in mass production [2] and provides remanent induction above $B_r = 1.0 \text{ T}$ together with extreme demagnetization stability. The development of cheap ferrite magnets has reached remanent induction of $B_r = 0.4 \text{ T}$ in the vicinity of the theoretical maximum ($B_r < 0.46 \text{ T}$).

Due to reduced dimensional tolerances in micromotors the machining of sintered magnets has become expensive. A new group of RE Co and Sr O plastic magnets has been introduced into mass production (fig. 3), which is inferior in magnetic characteristics, but which needs no final machining even when using complex geometrical structures.

Research efforts to substitute the sheet iron of the magnetic circuit by die-casted or sintered powdered material have reached an interesting level (fig. 4). The break-even of these new materials will depend on reducing the costs by mass production. Such magnetic materials might revolutionize machine construction in the near future. Because of the inherent low relative permeability of these materials ($10 \leq \mu_r \leq 100$) they will be used only in

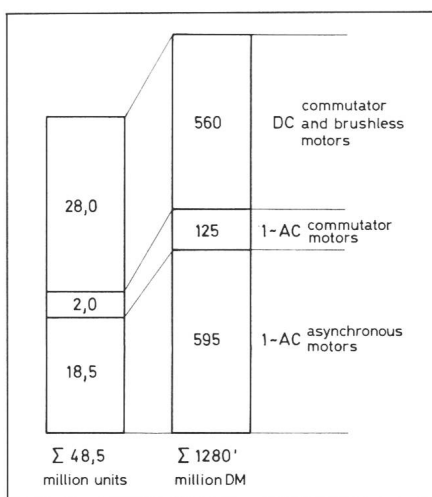


Fig. 1 Market of small electric machines ($P_1 \leq 375$ W), FRG 1982 [1]

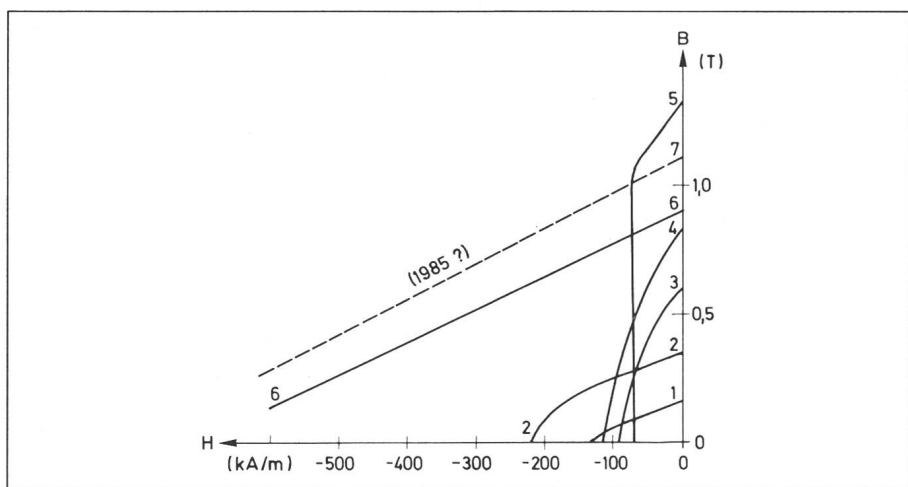


Fig. 2 Characteristics of permanent magnets

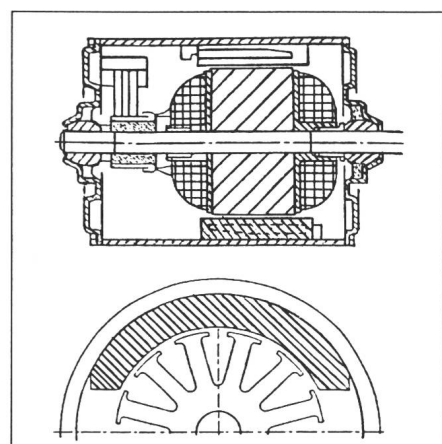


Fig. 5 PM-excited DC motor with shell-type magnets

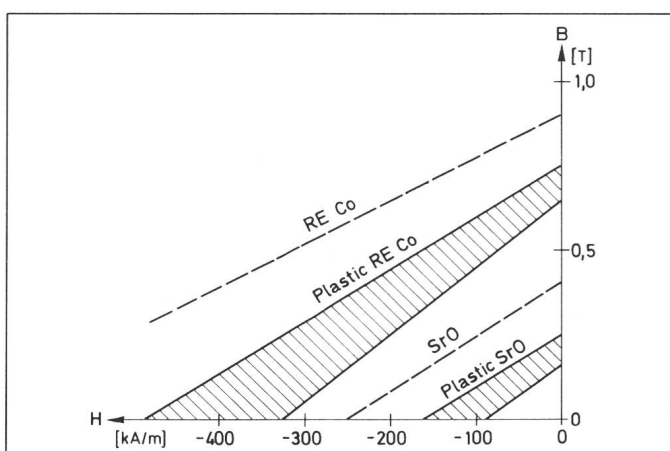


Fig. 3 Properties of plastic magnets

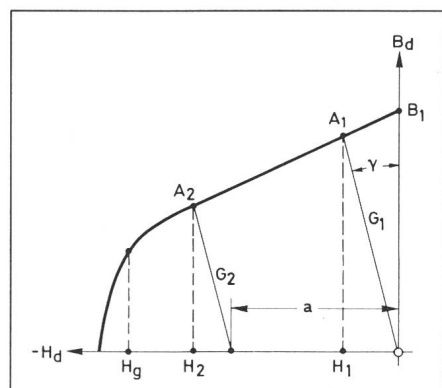


Fig. 6 Stable operation of permanent magnets [4]
 B_d , H_d direct axis field components

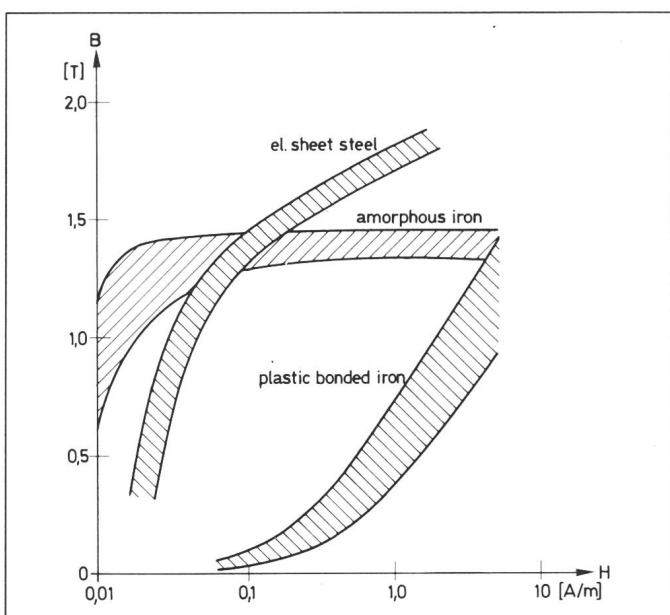


Fig. 4 Characteristics of soft magnetic materials

very small motors ($P_1 \leq 20$ W) with high frequencies of the magnetic field ($f \geq 400$ Hz). Moreover, replacing the sheet iron by powdered iron will reduce the output of these machines [3], the derating reaching about 30%.

3. DC-Commutator Motors with Permanent-Magnet (PM) Excitation

DC motors with mechanical commutator and ratings up to $P_1 = 300$ W are built with shell-type permanent magnets and tubular yoke (fig. 5). If the B and H fields coincide with the main (d-) axis of an anisotropic magnet material, the characteristics of the permanent magnet can be described in terms of $B_d = B_d (H_d)$ according to fig. 6. A rotor excitation displaces the working point from no-load situation

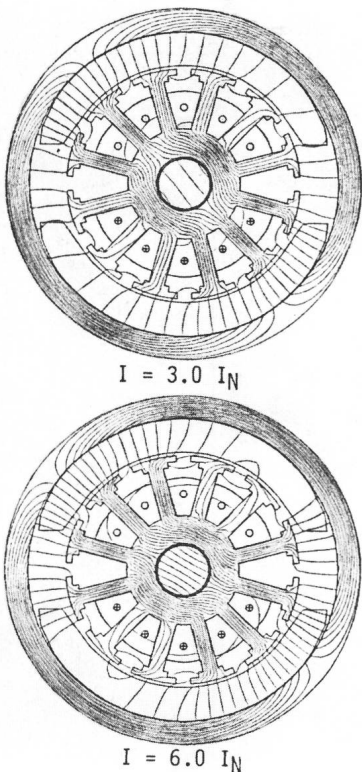


Fig. 7 Field distribution of a DC motor with permanent magnet at stand-still [6b]

A_1 to load situation A_2 ; the maximum permissible load may be calculated from the limiting value H_g .

Maximum demagnetization occurs on the trailing edge of the magnet under blocking conditions. As the permeability of the permanent magnet is very low and as the stator is dimensioned for normal load only, the assumption of fields in d-direction only is not valid, as shown in figure 7. With $I = 3 \text{ A}_N$ the B -field begins to deviate from d-direction, with $I = 6 \text{ A}_N$ the B -field even changes direction, thereby irreversibly demagnetizing the magnet.

If we consider an arbitrary situation of field deviation according to figure 8, showing a small angle α between flux density B_1 and d-axis (fig. 8a), we can calculate the corresponding field intensity H_1 at this point by using the d-and q-axis characteristics of the permanent magnet [4]. Permeability being very low, even a small amount of q-axis flux density B_{q1} leads to a high amount of q-axis field intensity H_{q1} (fig. 8b). Therefore the resulting field intensity H_1 is high and has an important q-axis or tangential component.

In order to analyse stability of the permanent magnet at blocking rotor, further information is required concerning the d-axis stability behaviour

Fig. 8
Field distribution in anisotropic permanent magnets

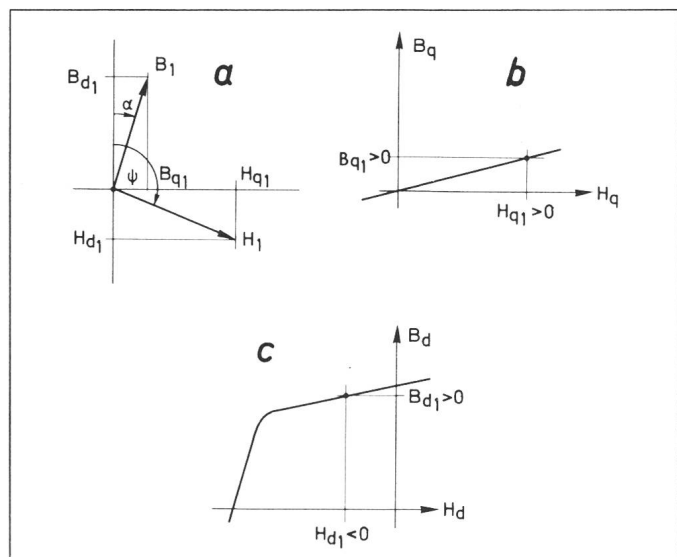
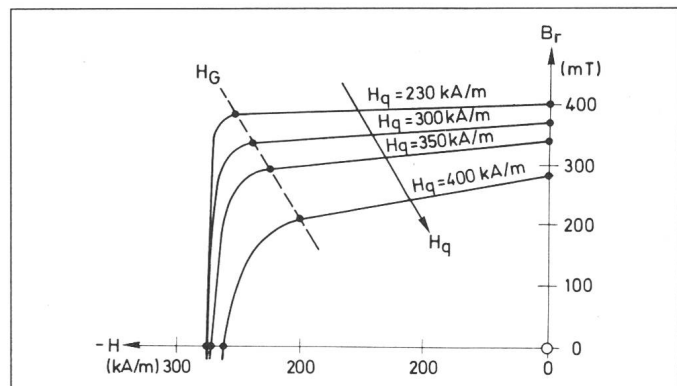


Fig. 9
Quadrature axis stability of anisotropic permanent magnets [5]



of the permanent-magnet material under quadrature axis field $H_q > 0$. Figure 9 shows the degradation of magnetic stability in the presence of quadrature axis fields.

For small values of the q-axis field intensity H_q there is no influence to the d-axis characteristics of the magnet. Exceeding a certain limiting value—here about 250 kA/m—the d-axis characteristic is rapidly degraded. For the purpose of field calculations one has to describe this behaviour properly.

In figure 10 a material model is shown, which was used in a more refined form by [6]. The well-known d-axis characteristic with constant parameters μ_{rd} , B_r and μ_{rq} is valid only for field intensity values below the material-dependent limiting value H_g . This limiting value is a function of the angle ψ between field intensity H and d-axis. With ideal magnets the limiting value H_g would follow the dashed line, which means that the d-axis characteristic is not influenced by q-axis fields. With real magnets, this limiting value is much lower, as shown by the full

line, because a q-axis field demagnetizes the d-axis. Magnetic materials with high stability against q-axis fields therefore become important with newly developed high remanence materials.

The design of a PM-excited commutator motor requires a compromise between high performance, which leads to a PM material with high remanence B_r , and stability against locked rotor currents, which leads to a material with high coercivity B_{Hc} . Mass-produced ferrite magnets cannot offer both features.

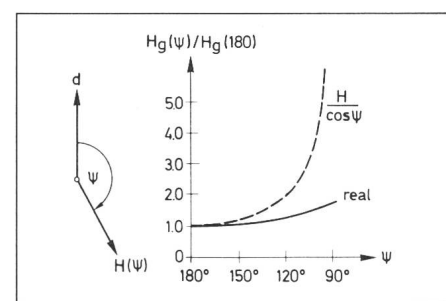


Fig. 10 Permanent magnet material model

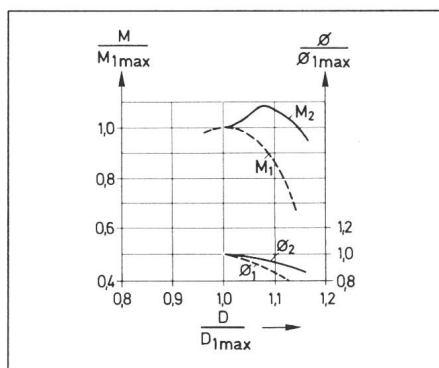


Fig. 11 Optimal rotor dimensions with composite magnets [6]

Index 1,2 correspond to material 1 resp. 2

M torque
 Φ magnetic flux
D rotor diameter

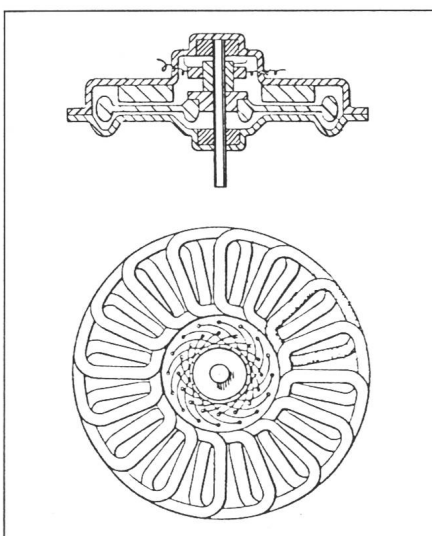


Fig. 12 Disc-type DC motor
(Matsushita Electric Industry Co., Japan)

As the stability of the permanent magnet is only a problem limited to the trailing edge, it is possible to build such a magnet from two different materials [7]. Material 1, which constitutes the greater part of the magnet, has high remanence B_r , but rather poor coercivity, and will provide the greater part of the main flux. Material 2, which has high coercivity, secures stability against demagnetization near the trailing edge, contributing a minor part to the main flux. Careful optimization of size and properties of the magnetic materials 1 and 2 can lead to a 10% improvement in blocking capability, if one is willing to adjust the rotor diameter to the optimal point (fig. 11).

For low-power drives in the VCR market¹⁾ disc-armature PM motors are widely used. Fig. 12 shows a typical layout with resin-bonded armature coils. Such motors provide very low torque ripple due to the lack of a toothed armature core, but efficiency is fairly modest and the automatization of the armature connections causes problems.

Whereas the low power range ($P_1 \leq 300$ W) is exclusively equipped with permanent-magnet excitation, higher power levels show problems at blocking condition because of instability against demagnetization. Stator pole shoes are to be used as shielding means against armature excitation, if there is no possibility of current limitation.

DC servomotors with ferrite-magnet excitation and current limitation are

standard drives for machine tools [8], even with shell-type magnets. Nominal torques range from 1 Nm up to 120 Nm, but overload torque is limited with increasing speed because of commutation problems (fig. 14).

4. Brushless DC Motors

Basically a brushless (BL) DC motor is an AC synchronous motor and his stator currents are commutated according to the rotor position in such a way, that maximum output torque is obtained at a given speed.

Accordingly the BL motor can be investigated as a m -phase synchronous motor with rectangular waveform stator voltages [9]. The resulting torque curves are given in figure 13. Torque characteristic C_1 is nonoptimal and corresponds to a fixed commutation angle, which is optimal for very low speeds. Torque characteristic C_2 is optimal and corresponds to a speed-dependent advanced commutation an-

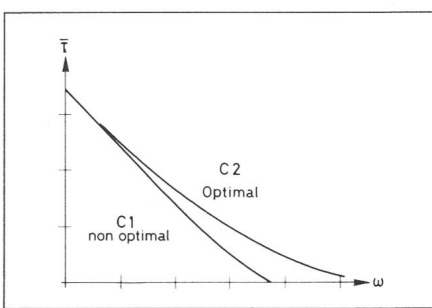


Fig. 13 Characteristics of BL motors
 \bar{T} Torque mean value

gle. The electrical time constant of a small BL motor is very short (typically $\tau_e \leq 10$ ms). So the torque characteristics tend to become straight lines, and the difference between nonoptimal and optimal commutation angle is negligible.

A major asset of the conventional DC motor is his low cogging torque. The BL motor normally has $m = 3$ and therefore tends to produce high torque ripple if stator currents are kept constant and the back EMF varies sinusoidally with time. By arranging winding distribution and air gap field in order to obtain trapezoidal back EMF [10] it is possible to produce with DC stator currents a torque with negligible ripple at low speed. So there are virtually no differences in the behaviour of conventional and brushless DC motors [11].

With increasing power output the electrical time constant τ_e of the BL motor increases and the motor has to be considered as a synchronous motor fed with variable frequency [12]. If the current vector of a BL motor is position-controlled to magnetize in the q -axis, maximum torque and minimum losses occur. To extend the working range beyond the voltage limitation of the inverter, the current position can be moved away from the q -axis so that the no-load speed increases.

Three-phase six-pole BL servomotors are in production [13] and offer superior performance as compared to commutator DC motors. RE Co segments are arranged on the rotor surface for PM excitation, and the stator is skewed to provide a small cogging torque. Nominal torques range from 1 to 55 Nm. The torque characteristics of the BL servomotor (fig. 14, full lines)

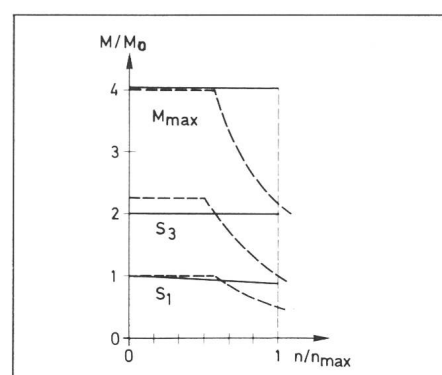


Fig. 14 Torque characteristics of PM servomotors
— BL Servo
- - - DC Servo

1) VCR = Video Cassette Recorder

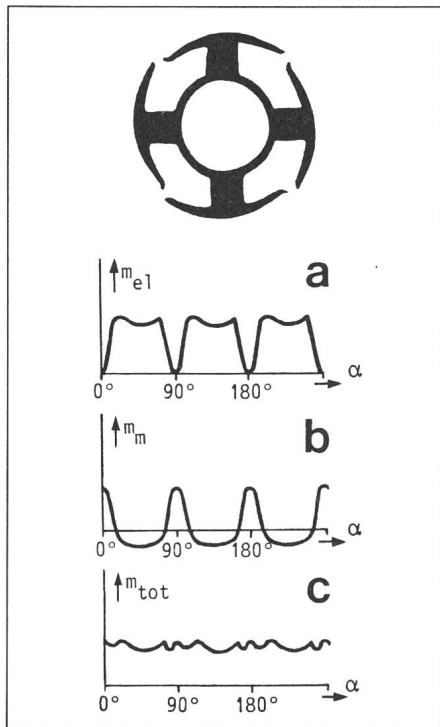


Fig. 15 Single-phase BL motor with additional reluctance torque [15]

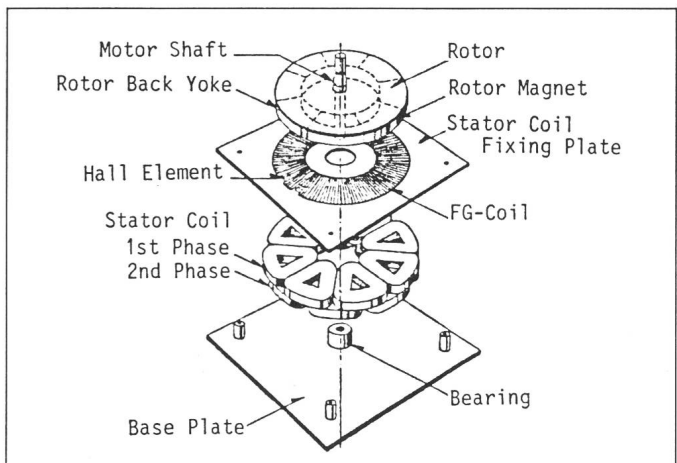
m_{el} electrical torque
 m_m cogging torque

show practically no reduction with increasing speed, whereas the torque characteristics of commutator servomotors (fig. 14, dashed lines) are restricted by commutation limits in the overload region.

Very small BL motors frequently are designed with a single stator phase ($m = 1$) to reduce the cost of electronics. To provide starting torque at every possible rotor position and to minimize torque ripple, a non-uniform air gap produces a cogging torque, according figure 15b [14], which fills the gaps between the electrically energized torque (fig. 15a). As the electromechanical torque and cogging torque have to be aligned close-fitting, the torques of figure 15 are valid only for a given excitation level, e.g. the nominal load and speed. Therefore motors of this kind show difficulties with their starting torque.

To avoid these disadvantages, a constant air gap and a non-uniform rotor magnetization [14] may be used. Coil span and effective pole width of the magnets are equally 120° (electrical degrees), and a constant torque is provided over a position angle of 240° . A motor of this type has the desired overload capacity, but is rather poor in his efficiency because of the small chord-

Fig. 16
Axial flux BL motor
(Daido Corp., Japan)



ing factor both of winding and magnet.

In the field of floppies and VCRs an increasing number of slim-line BL motors is needed. Figure 16 shows an axial air gap with a disc-type PM rotor leading to very flat motors. The stator windings and position sensors are incorporated in the etched circuit board. Sheet coil techniques have been developed to avoid wire windings completely.

lar splitted stator windings the stator voltages become unipolar DC pulses and the cost of stator electronics is decreased. Half-step operation is possible, if one allows for pulsating motor torques. As sheet-metal stators have high iron losses, this type of motor is used only for medium stepping frequencies up to $f_s \leq 1000 \text{ s}^{-1}$.

Hybrid or HY stepping motors combine the Vernier principle of reluctance motors and the homopolar excitation of the interference machine (fig. 18). The stator and sometimes the rotor are laminated structures; therefore these motors allow high stepping frequencies up to $f_s = 10000 \text{ s}^{-1}$ and high torques up to $M_H \leq 2...5 \text{ Nm}$. As the stator and rotor yoke flux is both radial and axial, the axial magnetic conductivity of the yokes has to be taken into account [17].

Operating a stepping motor near or below its natural frequency can induce stability problems [18]. As PM stepping motors have no damper windings on their rotors, stepping motors also show an inherent instability in the slew region [19], if external damping is very low. Short-term operation up to $T \leq$

5. Step motors

Positioning devices with small load torque (up to 0.5 Nm) are equipped with stepping motors, which in recent years have proved to be both economical and reliable. Table I shows some characteristics of three standard types: sheet-metal PM motors with heteropolar rotor excitation, reluctance motors with unexcited rotor and hybrid motors with homopolar excited reluctance rotor [15].

Sheet-metal PM motors have two stator phases in axially separated motor systems (fig. 17). By applying bifil-

Types of step motors

Table I

	Sheet-metal PM, heteropolar excited	Hybrid reluctance motor, homopolar excited	Reluctance motor nonexcited
Single Stator	$90^\circ \geq \alpha_s \geq 30^\circ$ $M_H \leq 0,5 \text{ Nm}$ $m = 2,3$	$3,6^\circ \geq \alpha_s \geq 0,9^\circ$ $M_H \leq 2 \text{ Nm}$ $m = 2$	$15^\circ \geq \alpha_s \geq 0,2^\circ$ $M_H \leq 0,5 \text{ Nm}$ $m = 3,4$
Multi-Stator	$22^\circ \geq \alpha_s \geq 3,75^\circ$ $M_H \leq 0,25 \text{ Nm}$ $m = 2$	$\alpha_s = 1,8^\circ$ $M_H \leq 0,5 \text{ Nm}$ $m = 2$	$15^\circ \geq \alpha_s \geq 1^\circ$ $M_H \leq 0,5 \text{ Nm}$ $m = 3$

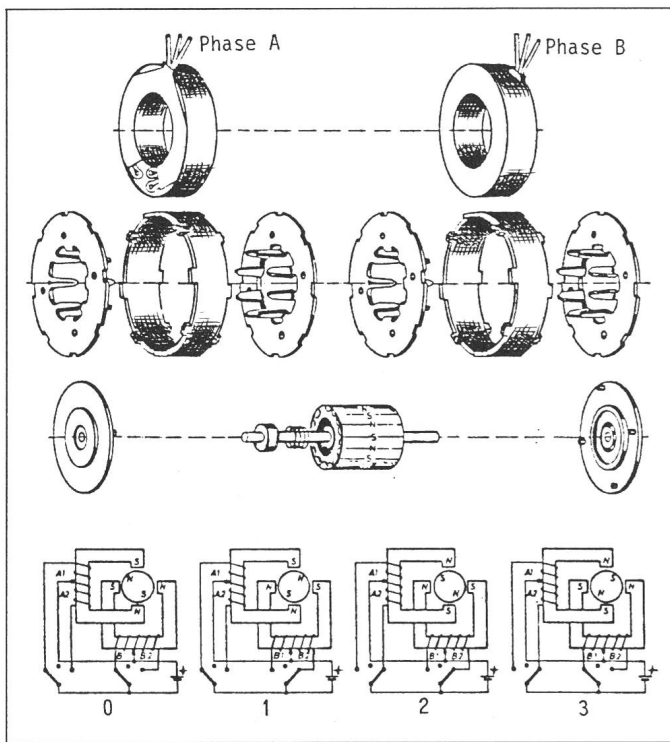


Fig. 17
Sheet-metal PM
stepping motor

$$p = 8 \\ m = 2 \\ \alpha = \frac{350^\circ}{2 \cdot p \cdot m} = 11,25^\circ$$

(Nach einem Vortrag von E. Traeger, Techn. Akademie Esslingen, Mai 1984)

[5] J. Koch: Über die Optimierung von permanentmagnetisch erregten Gleichstrommotoren bei Verwendung von Mehrstoffmagneten. Dissertation der Universität Stuttgart, 1982.

[6a] H. Gutt und Q. N. Tran: Über die Berechnung der Ankerrückwirkung von dauerstromerregten Gleichstromkleinmotoren mit Schalenmagneten und über Möglichkeiten der Leistungssteigerung. ETZ-Archiv 5(1983)7, S. 215...219.

[6b] Q. N. Tran: Über die Berechnung von permanentmagnetisch erregten Kleinmotoren. Dissertation der Technischen Hochschule Stuttgart, 1984.

[7] A. Mohr: Auswirkungen hochkonzentrierter Permanentmagnetmaterialien auf das Anlaufverhalten von Gleichstrommotoren. ETZ-Archiv 5(1983)12, S. 385...391.

[8] H.-J. Fischer und H. Riedel: Vorschubantriebe für Werkzeugmaschinen. Siemens-Energie-technik 3(1981)8/9, S. 276...280.

[9] J. Tal: Optimal commutation of brushless motors. Proceedings of the eleventh Annual Symposium Incremental Motion Control System and Devices 1982; p. 49...54.

[10] J. Tomasek: Brushless servo motor-amplifier optimization. Proceedings of the eighth Annual Symposium Incremental Motion Control System and Devices 1979; p. 279...291.

[11] N. Wave: Evolution des moteurs électriques pour la robotique moderne. Bull. SEV/VSE 75(1984)12, p. 673...675.

[12] H. Grotstollen: Die polradorientierte Regelung eines Drehstrom-Servoantriebes mit dauer-magnetisch erregtem Synchronmotor. ETZ-Archiv 5(1983)11, S. 339...346.

[13] K. Lasermann und H. Zander: Drehstrom-Vorschubantrieb für Werkzeugmaschinen. Siemens-Energie-technik Produktinformation 3(1983)2, S. 45...46.

[14] R. Müller: Gleichstrommotoren mit elektronischem Kommutator. VDI-Berichte 482(1983), S. 3...10.

[15] H. P. Kreuth: Stationäre und dynamische Betriebsdaten von Schrittmotoren. VDI-Berichte 482(1983), S. 91...96.

[16] I. E. D. Pickup and A. P. Russell: Nonlinear model for predicting settling time and pull-in rate in hybrid stepping motors. Proc. IEE 126(1979)4, p. 307...312.

[17] Q.-S. Gu: The air gap field of a synchronous inductor motor with permanent magnetic rotor. IEE Conference Publication No. 202: Small and special electrical machines; p. 55.

[18] P. J. Lawrence and I. E. Kingham: Resonance effects in stepping motors. Proc. IEE 124(1977)5, p. 445...448.

[19] A. J. C. Bakhuizen and J. H. Wouterse: Slew-region instability of permanent-magnet steppers. Proc. IEE 125(1978)2, p. 121...124.

[20] C. K. Taft and R. G. Gauthier: Stepping motor failure model. IEEE Trans. IECI 22(1975)3, p. 375...385.

[21] C. K. Taft and R. G. Gauthier: The phase plane as a stepping motor system design tool. Proceedings of the first Annual International Motorcon '81 Conference, June 10...13, 1981, Chicago/Illinois/USA; paper 6A, p. 278...288.

0.5 s is feasible, but long-term stability can only be provided with additional mechanical damping.

Optimal stepping programs are developed by trial and error; further research efforts in this field are required. Phase plan methods have been applied to develop stepping strategies (fig. 19), but the stability boundaries

are only valid for constant-current drive.

Literatur

- [1] Produktionsstatistik für Kleinmotoren. Frankfurt a.M., ZVEI, 1983.
- [2] A. L. Robinson: Powerful new magnet material found. Science 223(1984)4639, p. 920...922.
- [3] H.-J. Wahlen und H. Weh: Eisenpressteile als Statormaterial für elektrische Maschinen. ETG-Fachberichte 8(1981), S. 84...87.
- [4] A. Mohr: Die Ankerquerfeldbeanspruchung von Permanentmagnetsegmenten in kleinen Gleichstrommotoren aus der Sicht von Theorie und Praxis. ETZ-Archiv 5(1983)1, S. 3...10.

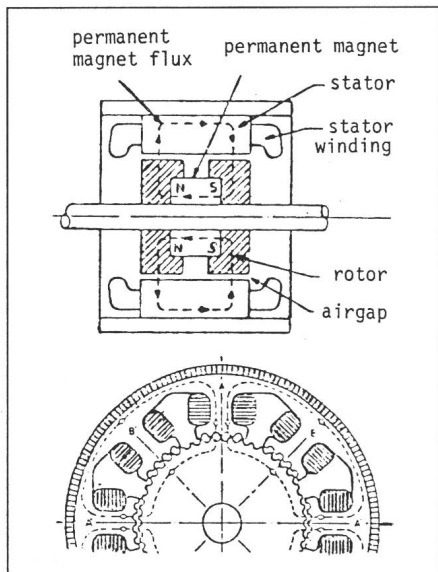


Fig. 18 Hybrid PM stepping motor [16]

Fig. 19
Phase plan
representation of an
optimal stepping
strategy [20; 21]

